Biochimica et Biophysica Acta 1843 (2014) 2114–2121

Contents lists available at ScienceDirect

Biochimica et Biophysica Acta

journal homepage: www.elsevier.com/locate/bbamcr

miR-141-3p inhibits human stromal (mesenchymal) stem cell proliferation and differentiation

Weimin Qiu [a,*], Moustapha Kassem [a,b]

[a] Molecular Endocrinology Laboratory (KMEB), Department of Endocrinology, Odense University Hospital, J.B. Winsløws Vej 25, 1, DK-5000 Odense C, Denmark
[b] The Danish Stem Cell Center (DanStem), University of Copenhagen, Copenhagen, Denmark.

ARTICLE INFO

Article history:
Received 14 January 2014
Received in revised form 6 June 2014
Accepted 9 June 2014
Available online 14 June 2014

Keywords:
Human stromal (mesenchymal) stem cell
miRNA
Cell proliferation and differentiation
Wnt signaling
CDC25A

ABSTRACT

Wnt signaling determines human stromal (mesenchymal) stem cell (hMSC) differentiation fate into the osteoblast or adipocyte lineage. microRNAs (miRNAs) are small RNA molecules of 21–25 nucleotides that regulate many aspects of osteoblast biology. Thus, we examined miRNAs regulated by Wnt signaling in hMSC. We identified miRNA (miR)-141-3p as a Wnt target which in turn inhibited Wnt signaling. Moreover, miR-141-3p inhibited hMSC proliferation by arresting cells at the G1 phase of the cell cycle. miR-141-3p inhibited osteoblast differentiation of hMSC as evidenced by reduced alkaline phosphatase activity, gene expression and in vitro mineralized matrix formation. Bioinformatic studies, Western blot analysis and 3'UTR reporter assay demonstrated that cell division cycle 25A (CDC25A) is a direct target of miR-141-3p. siRNA-mediated knock-down of CDC25A inhibited hMSC proliferation and osteoblast differentiation. In summary, miR-141-3p acts as a negative regulator of hMSC proliferation and osteoblast differentiation. Targeting miR-141-3p could be used as an anabolic therapy of low bone mass diseases, e.g. osteoporosis.

1. Introduction

microRNAs (miRNAs) are a large family of evolutionarily conserved, small (approximately 22 nucleotides in length) and non-coding RNA molecules [1,2]. To date, more than 1400 miRNAs have been identified in human cells, and each is predicted to regulate several target genes [3,4]. miRNAs regulate gene expression either at the posttranscriptional level by binding to the 3'UTR of target mRNAs, resulting in translational repression [5] or mRNA degradation [6,7], or at the transcriptional level by interacting with gene promoters to activate or repress gene expression [8,9]. miRNAs play critical roles in diverse biological and cellular processes including metabolism, differentiation and apoptosis. The physiological relevance of miRNA has also been demonstrated by the association of aberrant miRNA expression with a large number of human diseases including cancer, diabetes, neurological disorders, heart failure, pulmonary hypertension and autoimmune diseases due to dysfunction of their target genes [2]. Recent evidence demonstrates that miRNAs are regulators of osteogenesis during embryonic bone development as well as remodeling of adult bone tissue, a process that involves cell proliferation, differentiation and functional activity of bone cells [2,10]. For example, miRNA (miR)-138 has been demonstrated by our group to regulate osteoblast differentiation in vitro and in vivo [11], and a novel panel of miRNAs (OstemiR) were identified to target osteoblast differentiation-, stemness-, epigenetics-, and cell cycle-related genes [12].

Human bone marrow-derived stromal stem cells (hMSC, also known as skeletal stem cells and bone marrow mesenchymal stem cells) are a group of clonogenic and multipotent cells capable of differentiation into mesoderm-type cells, e.g. osteoblast, adipocyte and chondrocyte [13]. Alterations in the balance between osteoblast and adipocyte differentiation of MSC can lead to alterations in bone mass [14]. We have previously reported that high bone mass patients harboring the activating T253I mutation in Wnt coreceptor low-density lipoprotein receptor-related protein 5 exhibit increased bone mass and decreased bone marrow adipose tissue mass in iliac crest bone biopsies [15]. Additionally, we have demonstrated that this phenotype was caused by enhanced differentiation of hMSC by Wnt signaling into the osteoblastic, but not adipocytic, fate [15].

Several miRNAs have been reported to target Wnt inhibitors and thus activate Wnt signaling and bone formation. miR-29 promotes osteoblast differentiation through activation of Wnt signaling by a positive feedback loop, where miR-29 can be activated by Wnt signaling and targets Wnt inhibitors CTNNBIP1, DKK1, SFRP2 and Kremen2 [16–18]. miR-27 and miR-335 activate Wnt signaling and further stimulate osteoblast differentiation by targeting Wnt inhibitors APC and DKK1 respectively [19,20].

However, how Wnt signaling regulates the expression of miRNAs in hMSC is poorly characterized. In this study, we analyzed the expression of 88 miRNAs upon Wnt3a stimulation of hMSC by miRNA PCR array.

* Corresponding author at: Molecular Endocrinology Laboratory (KMEB), Department of Endocrinology, Odense University Hospital, Winsløwsparken 25.1, DK-5000 Odense C, Denmark. Tel.: +45 65504965; fax: +45 65503950.
E-mail address: wqiu@health.sdu.dk (W. Qiu).

http://dx.doi.org/10.1016/j.bbamcr.2014.06.004
0167-4889/

We identified miR-141-3p as a negative regulator of Wnt signaling, hMSC proliferation and osteoblast differentiation.

2. Material and methods

2.1. Cell culture and hMSC differentiation

The culture and differentiation of hMSC as well as preparation of Wnt3a conditioned medium (Wnt3a) and control conditioned medium (CCM) have previously been described [15]. For the current experiments we employed a human telomerized bone marrow derived stromal stem cells line: hMSC-TERT that has previously been described and expresses all markers of primary hMSC including in vivo bone formation [21,22]. We will refer these cells as hMSC in the manuscript. Conditioned media containing Wnt3a were prepared from murine L-cell overexpressing Wnt3a (ATCC, CRL-2647) and CCM were prepared from control L cell line (ATCC, CRL-2648). Cell culture and preparation of the conditioned media were performed as described by ATCC.

Mouse bone marrow-derived stromal cell line ST2 was maintained in RPMI-1640 (Invitrogen) containing 10% fetal bovine serum (FBS, Sigma) and 100 μg/ml streptomycin/penicillin (Invitrogen). HEK293T and MDA-MB231 human breast carcinoma cells were cultured in DMEM with 10% FBS and 100 μg/ml streptomycin/penicillin.

2.2. miRNA PCR array and miScript primer assay

hMSC were seeded in 6 cm dishes and treated with 20% Wnt3a or CCM for 24 hours. Total RNAs including miRNAs were isolated by miRNeasy mini kit (Qiagen), reverse transcribed by miScript II RT kit (Qiagen), and mature miRNAs were quantitated by miScript PCR system (Qiagen). Human miFinder miRNA PCR array (Qiagen) was performed on StepOnePlus real-time PCR system (Applied Biosystems) according to the manufacturer's instruction. To analyze the expression of a specific mature miRNA, miScript primer assay was performed. Universal primers for selected mature miRNAs were purchased from Qiagen, and their expression was analyzed by miScript PCR system.

2.3. Cell transfection

hMSC was reverse transfected with miRNA or siRNA by Lipofectamine™ 2000 (Invitrogen). Briefly, 1 pmol miRNA (Qiagen) or 5 pmol siRNA (Ambion) was mixed with 1 μl or 0.25 μl Lipofectamine 2000 in 10 ul or 50 ul serum free medium for 20 minutes at room temperature in 96-well plate. The cells were seeded at $6 \times 10^3/cm^2$ or to be approximately 70% confluent on the next day. The final concentration of miRNA and siRNA was 9 nM or 33 nM in a 96-well plate, these concentrations were also applied to other culture formats. The transfection efficiency of miR-141-3p was determined by miScript PCR system. To transfect miScript target protector, 225 nM final concentration was used.

2.4. Cell viability and cell cycle analysis

Cell viability was determined by CellTiter Blue reagent (Promega) as described previously [23]. For cell cycle analysis, hMSC were transfected with miRNA or siRNA in 6 cm dishes. After 24 hours, the cells were

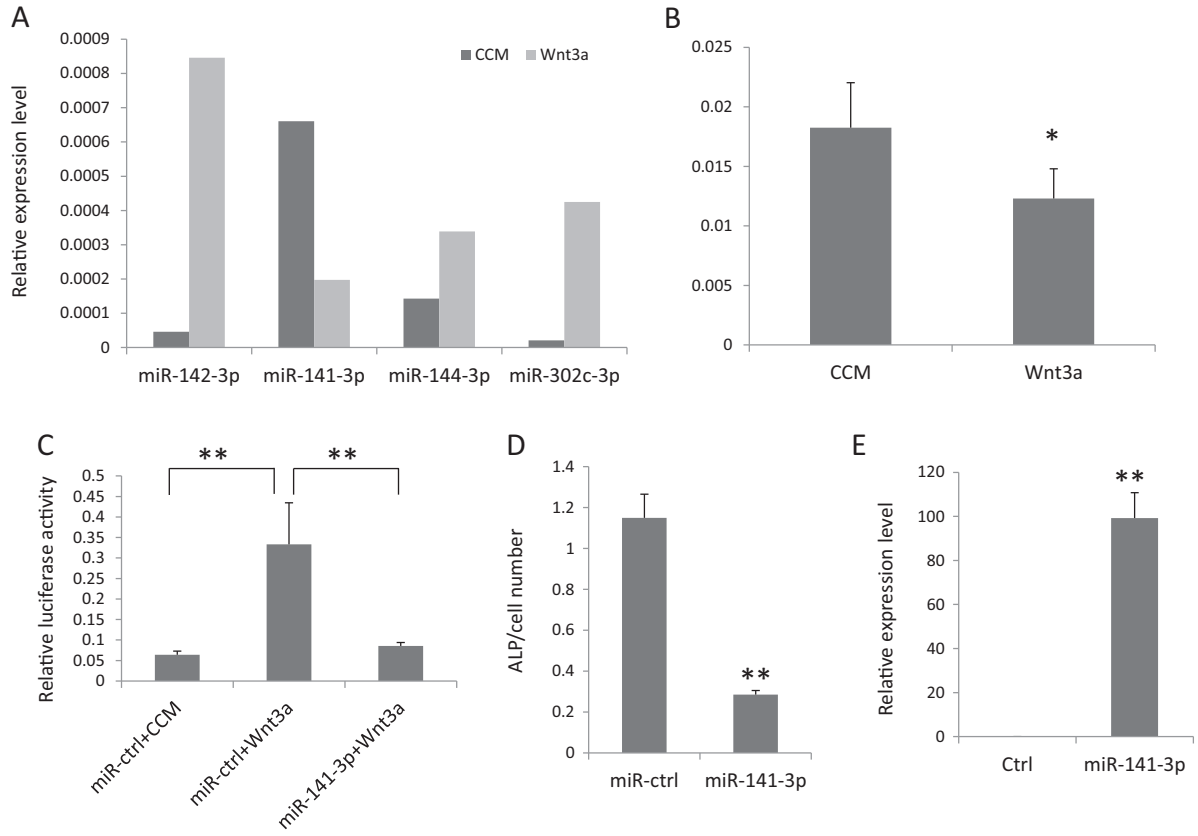

Fig. 1. The expression of miR-141-3p is inhibited by Wnt signaling. (A–B) hMSC were treated with Wnt3a conditioned medium (Wnt3a) or control conditioned medium (CCM) for 24 hours, and the expression of miRNAs was analyzed by human miFinder miRNA PCR array (A). The downregulation of miR-141-3p was further confirmed by miScript primer assay. Data are shown as mean + S.D., n = 5, * P < 0.05 (B). (C) Wnt reporter cell line was reverse transfected with 9 nM control miRNA (miR-ctrl) or miR-141-3p followed by treatment with 20% CCM or Wnt3a for 24 hours. The luciferase activity was measured by dual luciferase assay and presented as mean + S.D., n = 5, ** P < 0.005. (D) hMSC was reverse transfected, as above, followed by treatment with 20% Wnt3a for 7 days. ALP activity was normalized against cell number. Data are shown as mean + S.D., n = 8, ** P < 0.005. (E) hMSC was reverse transfected by 9 nM miR-141-3p as above, and mature miR-141-3p was quantitated by miScirpt primer assay. Nontransfected hMSC was used as control (Ctrl). Data are shown as mean + S.D., n = 3, ** P < 0.005.

treated in absence or presence of 0.1 μg/ml Nocodazole for 30 hours in order to arrest the cells in G2/M phase. The cells were subsequently trypsinized and washed with ice-cold PBS. 5×10^5 cells were fixed in 70% ice-cold ethanol at −20 °C for at least two hours and followed by treatment with 250 μl PBS containing 10 μg/ml RNase A and 20 μg/ml propidium iodide (PI) for 20 minutes. FACS analysis was performed on Cell Lab Quanta SC™ flow cytometer (Beckman Coulter), and data was analyzed by Kaluza software.

2.5. Cell apoptosis assay

For cell apoptosis assay, hMSC were transfected with miRNA in 10 cm dishes. Cells were collected after 48 hours, re-suspended in culture medium to 5×10^6/ml, stained with 40 nM MitoTracker® Red CMXRos (Invitrogen) for 30 min at cell culture condition for mitochondria activity. Then cells were washed by PBS, resuspended in PBS at 10^6/ml and stained with 100 nM YO-PRO®-1 (Invitrogen) on ice for 20 min for cell membrane permeability. In addition, apoptotic cell marker Caspase 3 was examined by Western blot analysis 48 hours following transfection.

2.6. Real-time qRT-PCR

hMSC differentiation marker expressions were determined by real-time qRT-PCR as described previously [15,23,24]. To determine the miR-141-3p effects on the expression on target genes, hMSC were transfected with miR-141-3p or control and gene expression was analyzed after 48 hours. Primers used in this study are: cell division cycle 25A (CDC25A) forward primer 5'-GATCTCAAGAGGAGTCTCCACC-3' and reverse primer 5'-TAAATCCTGATGTTTCCCAGC-3'; cyclin D1 (CCND1) forward primer 5'-AGCTGCTGCAAATGGAGC-3' and reverse primer 5'-GGGTCACACTTGATCACTCTGG-3'. GAPDH was used as internal control.

2.7. Alkaline phosphatase (ALP) activity assay and alizarin red S staining

ALP activity was quantitated as described [23]. For alizarin red S staining, cells were cultured in osteoblast induction medium for 12 days, washed with PBS, fixed with ice-cold 70% ethanol for 30 minutes and stained with 40 mM alizarin red S (pH 4.2) for 1 hour.

2.8. Immunoprecipitation and Western blot analysis

Cell were lysed in RIPA buffer (Sigma) containing 1 mM PMSF and 2 mM vanadate, and protein concentration was measured by Coomassie Plus® protein assay reagent (Pierce). A 600 ug protein was mixed with 50 ul Protein G-Agarose (Roche), incubated at 4 °C for 3 hours and centrifuged at 1000 g, 4 °C for 30 seconds. The supernatant was incubated with 2 ug rabbit anti-CDK2 antibody (sc-163, Santa Cruz) at 4 °C for 2 hours. A 50 ul Protein G-Agarose was added, and the mixture was incubated overnight. Immunoprecipitates were collected by centrifugation and washed in RIPA buffer for four times. The pellets were re-suspended in 40 μl NuPAGE® LDS sample buffer, boiled at 95 °C for 10 minutes and the supernatants collected for electrophoresis. Western blot analysis was performed on NuPAGE® SDS-PAGE gel system (Invitrogen) according to manufacturer's instruction. Antibodies used

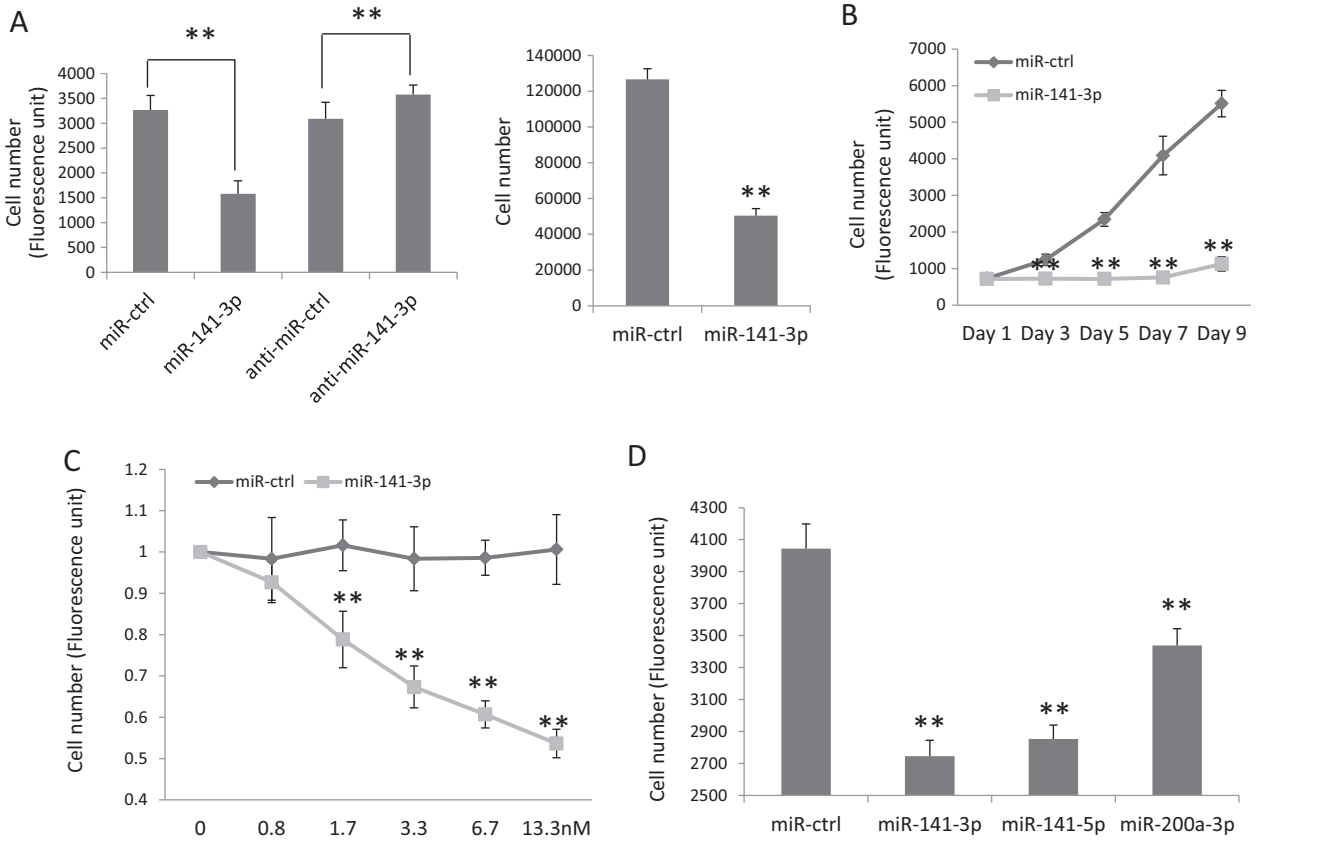

Fig. 2. miR-141-3p inhibits hMSC proliferation. (A) hMSC was reverse transfected with 9nM control miRNA (miR-ctrl), miR-141-3p, anti-miRNA control (anti-miR-ctrl) or anti-miR-141-3p. Cell number was analyzed by CellTiter Blue assay (Left) or hemacytometer (Right) after 48 hours. Data are shown as mean + S.D., n = 6–8, **P < 0.005. (B) hMSC was reverse transfected as above, and cell number was analyzed by CellTiter Blue assay from day 1 to day 9. Data are shown as mean ± S.D., n = 6, **P < 0.005. (C) hMSC was reverse transfected with 0–13.3 nM miR-ctrl or miR-141-3p. Cell number was analyzed as above after 48 hours. Data are shown as mean ± S.D., n = 7, **P < 0.005. (D) hMSC was reverse transfected, and cell number was analyzed as above. Data are shown as mean + S.D., n = 8. **P < 0.005.

in Western blot analysis were mouse anti-CDC25A (1:200, sc-7389, Santa Cruz), rabbit anti-CCNE2 (1:200, sc-22777, Santa Cruz), rabbit anti-CycD1 (1:200, sc-718, Santa Cruz), rabbit anti-Caspase-3 (1:1000, Cell Signaling), rabbit anti-CDK2 (1:1000, sc-163, Santa Cruz) and mouse anti-phosphotyrosine (1:2000, 05-321, Upstate). Mouse anti-α-tubulin (1:1000, T-5168, Sigma) was used as control.

2.9. 3'UTR-reporter assay

Luciferase reporter vector containing 3'UTR of human CDC25A was purchased from CD BioSciences Inc, USA. Mutations in miR-141-3p targeting site in 3'UTR of CDC25A (Fig. 4A) was introduced by using QuikChange Lightning Multi Site-Directed Mutagenesis Kit (Agilent Technologies) as instructed. HEK293T cells were reverse transfected by 100 ng reporter vector together with 13.3 nM miR-141-3p. Luciferase activity was measured by luciferase assay system (Promega) and normalized against protein concentration quantitated by Coomassie plus protein assay reagent (Pierce).

2.10. Bioinformatic and statistical analysis

To predicate the interaction between miR-141-3p and genes involved in cell cycle control, we first curated cell cycle genes expressed at basal level in our hMSC cells [22]. These genes were screened for miR-141-3p target sites by using Web tools: microRNA.org [25] and confirmed by using Pictar [26] and TargetScan [27]. The targeting sites of miR-141-3p in Wnt components were predicated as above, and known gene targets of miR-141-3p were retrieved from TarBase [28].

Differences between groups were examined using Student's *t*-test, and $P < 0.05$ was considered significant.

3. Results

3.1. miR-141-3p is down-regulated by canonical Wnt signaling

We have previously demonstrated that canonical Wnt signaling determines hMSC differentiation into osteoblast or adipocyte lineages and this was associated with activation of a novel Wnt target gene: TNFRSF19 as well as the non-canonical Wnt/JNK pathway [15,23,24]. Here, we examined the hypothesis that Wnt signaling mediates its regulatory effects on hMSC through regulation of miRNAs. We compared the expression of 88 miRNAs in hMSC following Wnt3a stimulation by miFinder® miRNA PCR array. We observed that the levels of miRNAs: miR-142-3p, miR-144-3p and miR-302c-3p were increased and the levels of miR-141-3p were decreased (Fig. 1A). The inhibitory effect of Wnt3a on miR-141-3p expression was further confirmed in an independent miScript primer assay (Fig. 1B). To determine whether miR-141-3p affects Wnt signaling, we transfected a Wnt reporter cell line, established by stable infection of hMSC with lentivirus expressing TCF/LEF-Luc reporter (CLS-018 L, SABiosciences) as well as Renilla luciferase gene (GenTarget Inc.) as control, with miR-141-3p. Subsequently, the cells were treated with Wnt3a or CCM for 24 hours. As seen in Fig. 1C, overexpressing miR-141-3p strongly inhibited Wnt3a-induced luciferase activity. In addition, miR-141-3p inhibited Wnt3a-induced ALP activity (Fig. 1D). The transfection efficiency of miR-141-3p was confirmed by miScript primer assay (Fig. 1E).

3.2. miR-141-3p inhibits hMSC proliferation by arresting hMSC at G1

As seen in Fig. 2A, miR-141-3p significantly decreased cell proliferation 48 hours following transfection and anti-miR-141-3p increased cell proliferation. Significant inhibition of miR-141-3p on cell proliferation was observed during 9 days of culture (Fig. 2B) and was mediated

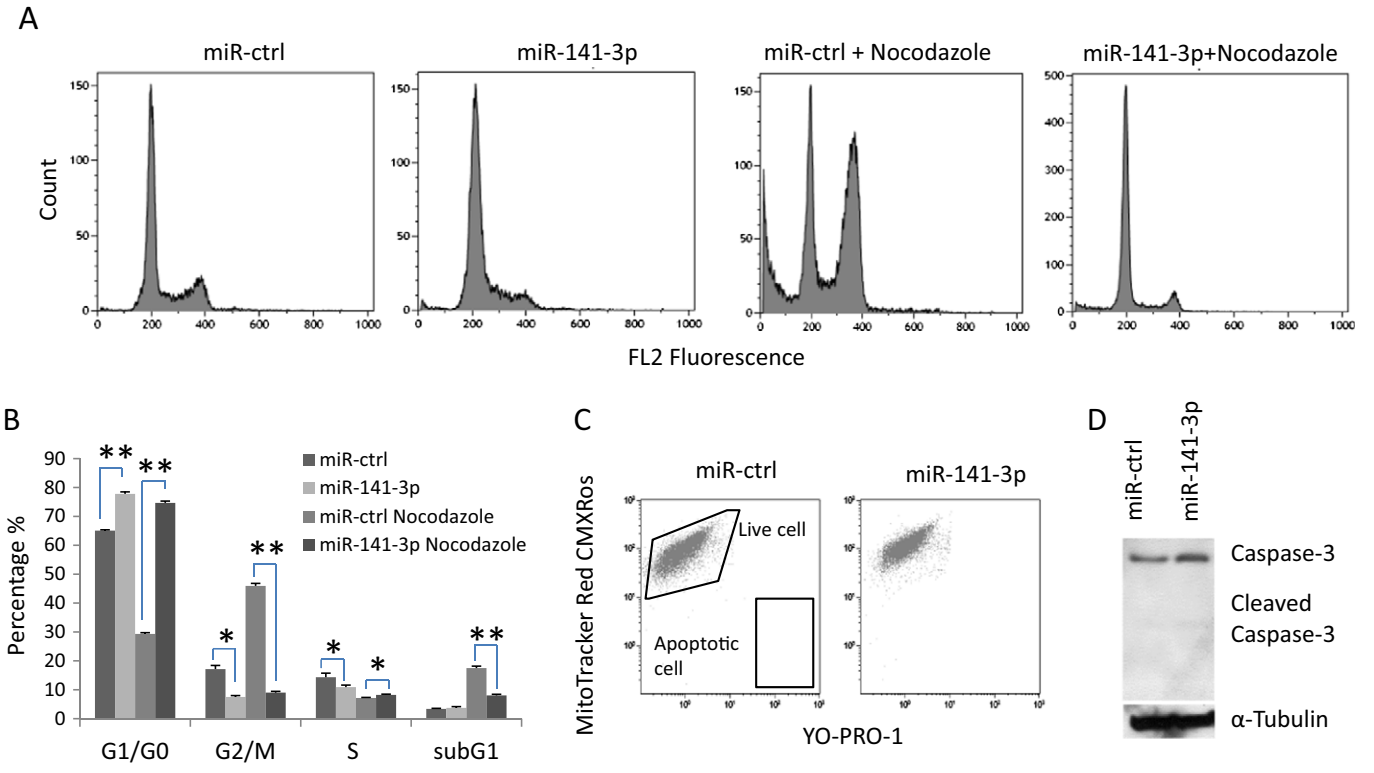

Fig. 3. miR-141-3p arrests hMSC at G1 phase. (A–B) hMSC was reverse transfected with 9 nM control miRNA (miR-ctrl) or miR-141-3p. The next day cells were treated with or without 0.1 ug/ml Nocodazole for 30 hours, and then cells were stained by propidium iodide for FACS analysis (A). Percentage of cells in G1/G0, G2/M, S and subG1 phase were calculated (B). n = 3, *P < 0.05, **P < 0.005. (C-D) miR-141-3p does not induce cell apoptosis. hMSC was reverse transfected as above. After 48 hours, cells were double stained by MitoTracker Red CMXRos and YO-PRO-1 for FACS (C), or cell were collected for Western blot analysis of Caspase-3 (D).

by concentrations of miRNA, used in transfection, as low as 1.7 nM ($P < 0.005$) (Fig. 2C). The inhibitory effect of miR-141-3p on cell proliferation was further confirmed in other cell models: primary human adipose tissue derived MSC, primary bone marrow derived MSC (Supplementary Fig. S1A and B) and mouse stromal stem cell line ST2 cells ($P < 0.005$). The effects on cell proliferation were less pronounced in HEK 293 T cells ($P = 0.035$) and was absent in the MDA-MB231 breast cancer line (Supplementary Fig. S1C). We also examined the effect of miR-141-5p, which is processed from the same stem loop structure, and miR-200a-3p, which belongs to the same miRNA precursor family associated with cell proliferation. All the three miRNAs inhibited cell proliferation, and miR-141-3p exhibited the strongest inhibitory effects (Fig. 2D).

To determine the cellular mechanisms of the inhibitory effects on cell proliferation, we examined the effects of miR-141-3p on cell cycle. Overexpression of miR-141-3p increased cells at G1/G0 from 65% to 78%, and correspondingly cells at G2/M decreased from 17% to 8%, and S phase cells decreased from 14% to 11% (Fig. 3A-B). Following 30 hours of treatment with 0.1 μg/ml Nocodazole, known to arrest cells at G2/M, FACS analysis revealed that 46% cells transfected with control miRNA (miR-ctrl) were arrested at G2/M and 36% cells were at G1/G0 and S phase. Conversely, 75% of the cells transfected with miR-141-3p remained at G1/G0 phase, which was similar to miR-141-3p transfected cells without Nocodazole treatment (Fig. 3A–B).

We also examined the effects of miR-141-3p on cell apoptosis by staining cells with MitoTracker Red CMXRos for mitochondria activity and YO-PRO-1 for cell permeability, which is known to be affected in apoptotic cells. FACS analysis did not demonstrate the presence of apoptotic YO-PRO-1 positive cells with reduced MitoTracker Red CMXRos signal (Fig. 3C). Additionally, Western blot analysis of Caspase-3 did not detect the apoptosis associated 17 kDa cleaved fragment (Fig. 3D). Thus, miR-141-3p inhibited hMSC proliferation by arresting cells in G1 phase without exerting effects on cell apoptosis.

3.3. CDC25A is miR-141-3p target gene

To explore how miR-141-3p arrests hMSC in G1 phase, we first curated 140 cell cycle related genes expressed in our hMSC cell line from a previous microarray study [22]. Among them, 18 genes were found to have at least one targeting site of miR-141-3p as evidenced from micorRNA.org resources (Supplemental Table 1). The miR-141-3p targeting site in the CDC25A gene was also confirmed by TargetScan

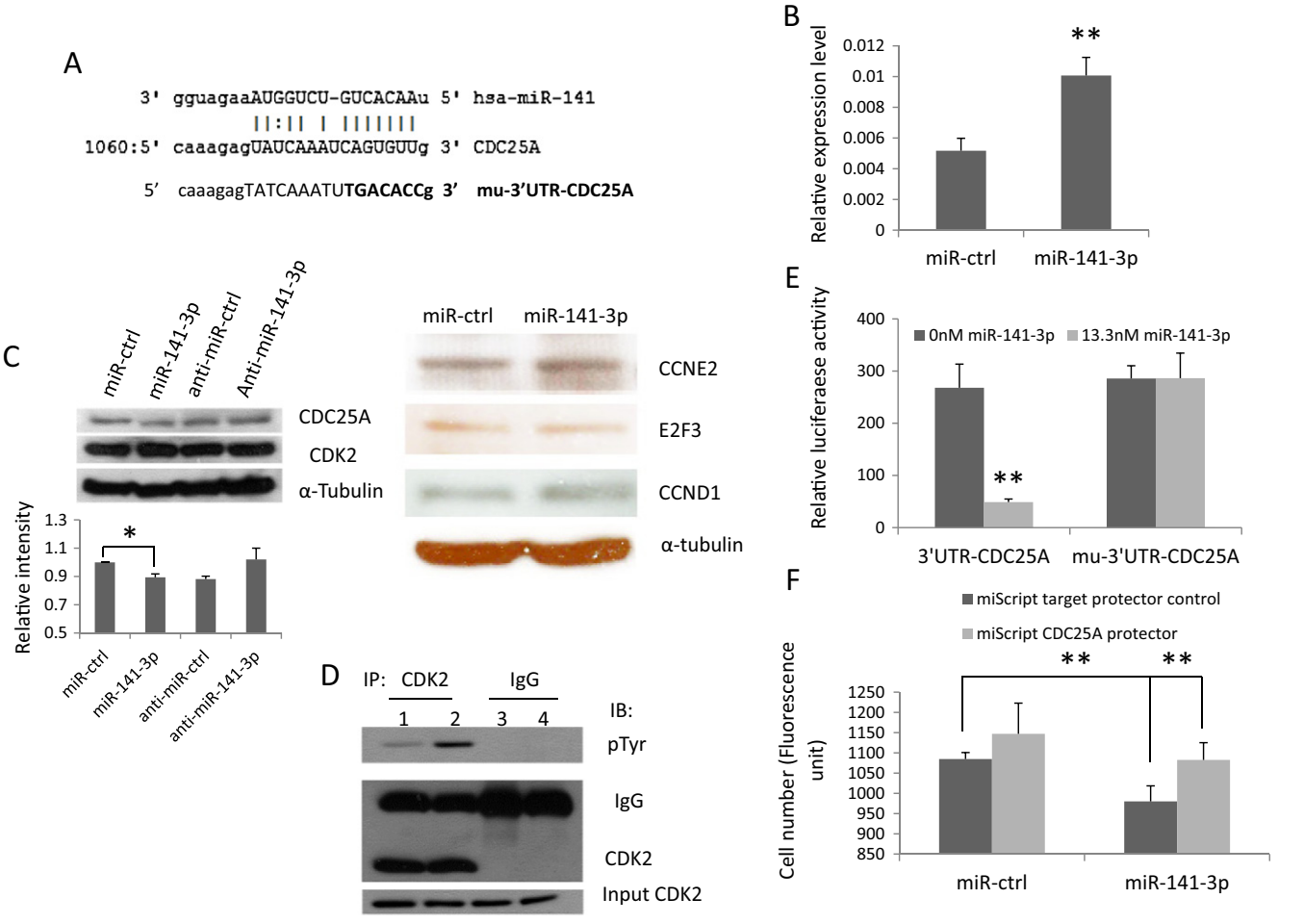

Fig. 4. miR-141-3p targets CDC25A. (A) Sequence alignment of miR-141-3p with CDC25A analyzed by microRNA.org. The 7 core nucleotides CAGUGUU in wild type 3'UTR of CDC25A were mutated to TGACACC (mu-3'UTR-CDC25A). (B–C) hMSC was reverse transfected with 9 nM control miRNA (miR-ctrl) or miR-141-3p for 48 hours, and expression of CDC25A was analyzed by real-time qRT-PCR and normalized against GAPDH ($n = 5$), $^{**}P < 0.005$ (B). The protein level of CDC25A as well as CDK2, CCNE2, E2F3 and CCND1 was analyzed by Western blot, and α-tubulin was used as internal control. The semi-quantitation of the expression of CDC25A was analyzed by ImageJ software and normalized against α-tubulin. The expression in cells transfected with miR.ctrl was set to 1. $n = 3$, $^{*}P < 0.05$ (C). (D) hMSC was reverse transfected as above, and proteins were collected 72 hours upon transfection. A 600 ng total protein was used for immunoprecipitation (IP) by anti-CDK2 antibody or IgG as control and then immunoblotted (IB) with anti-CDK2 antibody or anti-phosphotyrosine (pTyr). (E) HEK293T cells were reverse transfected with 100 ng wild type CDC25A 3'UTR reporter (3'UTR-CDC25A) or mu-3'UTR-CDC25A with 0 or 13.3 nM miR-141-3p and luciferase activity was measured, normalized by protein concentration and presented as mean + S.D., $n = 8$. $^{**}P < 0.005$. (F) hMSC was reverse transfected with 9 nM miR-ctrl or miR-141-3p with either 225 nM miScript target protector control or miScript CDC25A protector for 48 hours. Cell number was analyzed by CellTiter Blue assay. Data are shown as mean + S.D., $n = 7$, $^{**}P < 0.005$.

and PicTar (Fig. 4A). Western blot analysis revealed that miR-141-3p decreased CDC25A protein levels (Fig. 4C) but surprisingly increased its expression at the mRNA level (Fig. 4B). CDC25A is a phosphatase which activates the CDK2-cyclin E and CDK2-cyclin A complexes during G1-S transition by removing inhibitory phosphate groups from threonine-14 and tyrosine-15 of CDK2 [29]. Western blot analysis revealed that CDK2 was not affected by miR-141-3p (Fig. 4C). Further, CDK2 was immunoprecipitated from cells transfected with either miR-ctrl or miR-141-3p and probed for its phosphotyrosine level by anti-phosphotyrosine antibody. Consistent with decreased CDC25A protein levels by miR-141-3p, the phosphotyrosine level was higher in cells transfected with miR-141-3p (Fig. 4D). To confirm that CDC25A was a direct target of miR-141-3p, we employed a CDC25A 3'UTR luciferase reporter assay. Mutagenesis of miR-141-3p targeting site in CDC25A 3'UTR abolished the inhibitory effect of miR-141-3p (Fig. 4A, E). Furthermore, transfection of hMSC with miScript CDC25A protector rescued the inhibitory effect of miR-141-3p on cell proliferation (Fig. 4F).

Cyclin E2 (CCNE2) and E2F transcription factor 3 (E2F3) are also involved in G1/S transition and were predicated to have miR-141-3p targeting sites by miRNA.org, TargetScan and PicTar (Supplemental Table 1). However, Western blot analysis did not reveal reduced expression of these proteins following miR-141-3p overexpression (Fig. 4C). As a known target of miR-141-3p and in G1/S transition regulator, CCND1 is upregulated by miR-141-3p [30], which was also confirmed in our study (Fig. 4C). These data suggested that reduced CDC25A may be responsible for G1 arrest.

3.4. Knock down of CDC25A inhibits cell proliferation without significant G1 arrest

To further explore the function of CDC25A in inhibition of cell proliferation by miR-141-3p, we employed siRNA-based knock down of CDC25A. siCDC25A dramatically decreased the expression of basal CDC25A for more than 90% (Fig. 5A) and inhibited cell proliferation 48 hours after transfection (Fig. 5B). Cell cycle analysis by PI staining and FACS analysis did not demonstrate G1/G0 arrest by siCDC25A (Fig. 5C). These results suggested that CDC25A is a potential mediator of miR-141-3p inhibitory effects on cell proliferation.

3.5. miR-141-3p inhibits in vitro osteoblast differentiation of hMSC

We investigated the effect of miR-141-3p on in vitro osteoblast differentiation of hMSC. The expression of osteoblastic marker genes: ALP and collagen, type I, alpha 1 (COL1A1) as well as ALP enzyme activity were significantly reduced by miR-141-3p during 7 days osteoblast differentiation (Fig. 6A–B). The expression of runt-related transcription factor 2 (RUNX2) was increased by miR-141-3p at basal level ($P < 0.005$), unchanged during 4 days osteoblast differentiation but significantly decreased compared to cells transfected with miR-ctrl (Fig. 6A). In addition, miR-141-3p impaired in vitro mineralization as visualized by alizarin red staining (Fig. 6C).

To test for CDC25A as a mediator of the inhibitory effect of miR-141-3p on osteoblast differentiation, we knocked down CDC25A during in vitro osteoblast differentiation. CDC25A was reduced more than

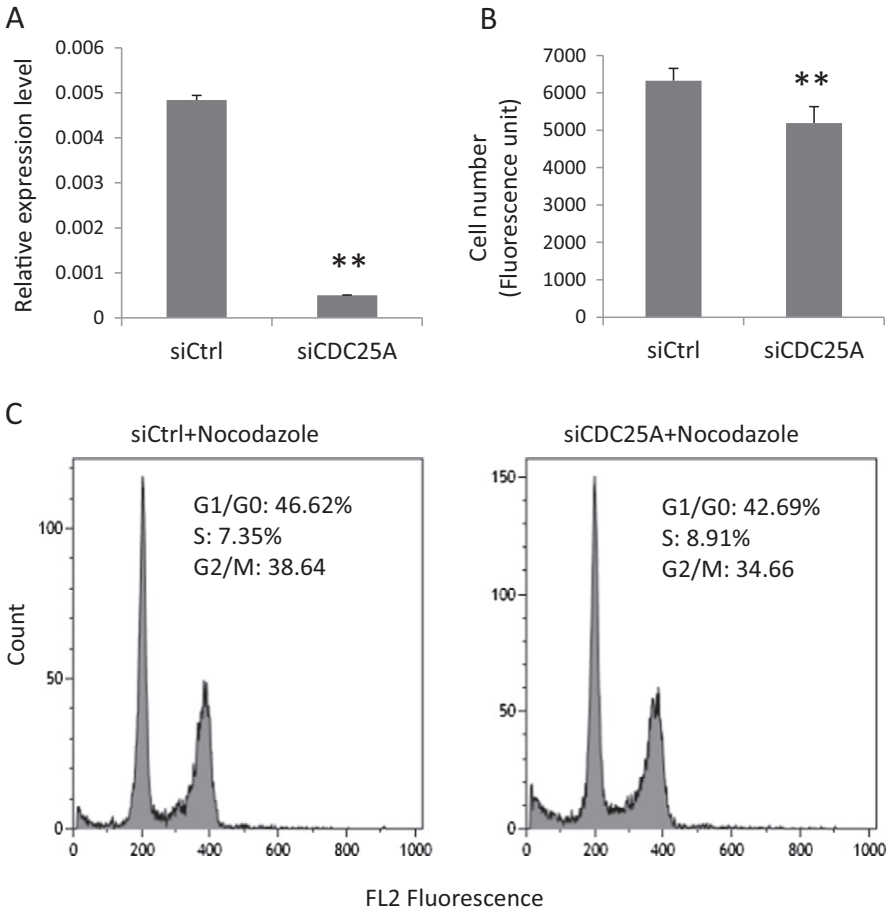

Fig. 5. Knock down CDC25A inhibits cell proliferation without G1 arrest. hMSC were reverse transfected with 33 nM control siRNA (siCtrl) or siRNA targeting CDC25A (siCDC25A) for 48 hours. (A) The expression of CDC25A was analyzed by real-time qRT-PCR and normalized against GAPDH. Data are shown as mean + S.D., n = 3, **P < 0.005. (B) Cell number was analyzed by CellTiter Blue assay after 48 hours. Data are shown as mean + S.D., n = 8, **P < 0.005. (C) Transfected cells were treated with 0.1 ug/ml Nocodazole for 30 hours, and then cells were stained by propidium iodide for FACS analysis. Data were shown as one of three independent experiments.

50% during 7 days osteoblast differentiation (Fig. 6D). We observed that siCDC25A inhibited the expression of RUNX2 and COL1A1, but did not change the expression of ALP (Fig. 6D). These results suggested that miR-141-3p inhibited in vitro osteoblast differentiation of hMSC through CDC25A.

4. Discussion

An expanding body of evidence demonstrates that osteoblast differentiation, osteoblast function and bone formation are controlled by miRNAs [2,10]. In the present study, we identified miR-141-3p as a novel Wnt signaling target, which exerts inhibitory effects on Wnt signaling. We also observed that part of the inhibitory effects of miR-141-3p on hMSC proliferation and differentiation is mediated by targeting CDC25A.

miR-141-3p belongs to the miR-200 family which consists of five miRNAs arranged into two clusters (miRs-200b/a/429 and miRs-200c/141) on chromosome 1 and 12 in humans [31]. miR-141 shares an identical seed sequence and differs by only one nucleotide with miR-200a [32]. Previous studies have shown that miR-141/miR-200 are involved in cancer development and metastasis. miR-141/mirR-200a are associated with ovarian tumorigenesis through targeting p38α and controlling oxidative stress response [5]. miR-141 targets PTEN, BRD3 and UBAP1, which affect AKT, Rb/E2F signaling and cell proliferation, respectively, in nasopharyngeal carcinoma [30]. The miR-200 family inhibits epithelial–mesenchymal transition, which is an essential initial step of cancer metastasis, by targeting E-cadherin, ZEB1 and ZEB2 [31]. Conversely, miR-200 has been reported to promote cancer metastasis capacity of a mouse breast cancer cell line as it enhanced mesenchymal to epithelial cell transition by targeting mouse Zeb2 [33]. Furthermore, miR-141/miR-200 family has been reported to inhibit cell proliferation in cancer cells [34,35]. However, in nasopharyngeal carcinoma cells, inhibition of miR-141 reduced cell viability and increased cell apoptosis [30]. In our study, we observed that miR-141-3p inhibited hMSC proliferation by arresting the cells at G1 phase without detectable effects on cell apoptosis. Both miR-141-3p and miR-200a-3p inhibited hMSC proliferation but miR-141-3p exhibited much stronger effects (Fig. 2D), suggesting that minor differences in nucleotide sequence existing between miR-141-3p and miR-200a-3p are relevant for their function.

We observed that miR-141-3p increased the expression of CDC25A in the mRNA level and decreased its expression in the protein level, suggesting that miR-141-3p affects gene expression on both a transcriptional and posttranscriptional level. miR141/miR-200a have also been reported to affect different aspects of bone biology. For example, miR141/miR-200a have been reported to inhibit BMP induced osteoblast differentiation in the mouse pre-osteoblastic MC3T3-E1 cell line by inhibiting osteoblastic transcription factor Dlx5 [36]. Additionally, elevated miR-141 levels were observed in serum from patients with prostate cancer and bone-metastasis, and serum levels of miR-141 were associated with the presence of increased bone lesions and were correlated with serum ALP activity [7]. In our study, miR-141-3p significantly reduced the expression of early osteoblast differentiation markers, including ALP, COL1A1 and RUNX2. Knocking down CDC25A inhibited hMSC proliferation and osteoblast differentiation, but this

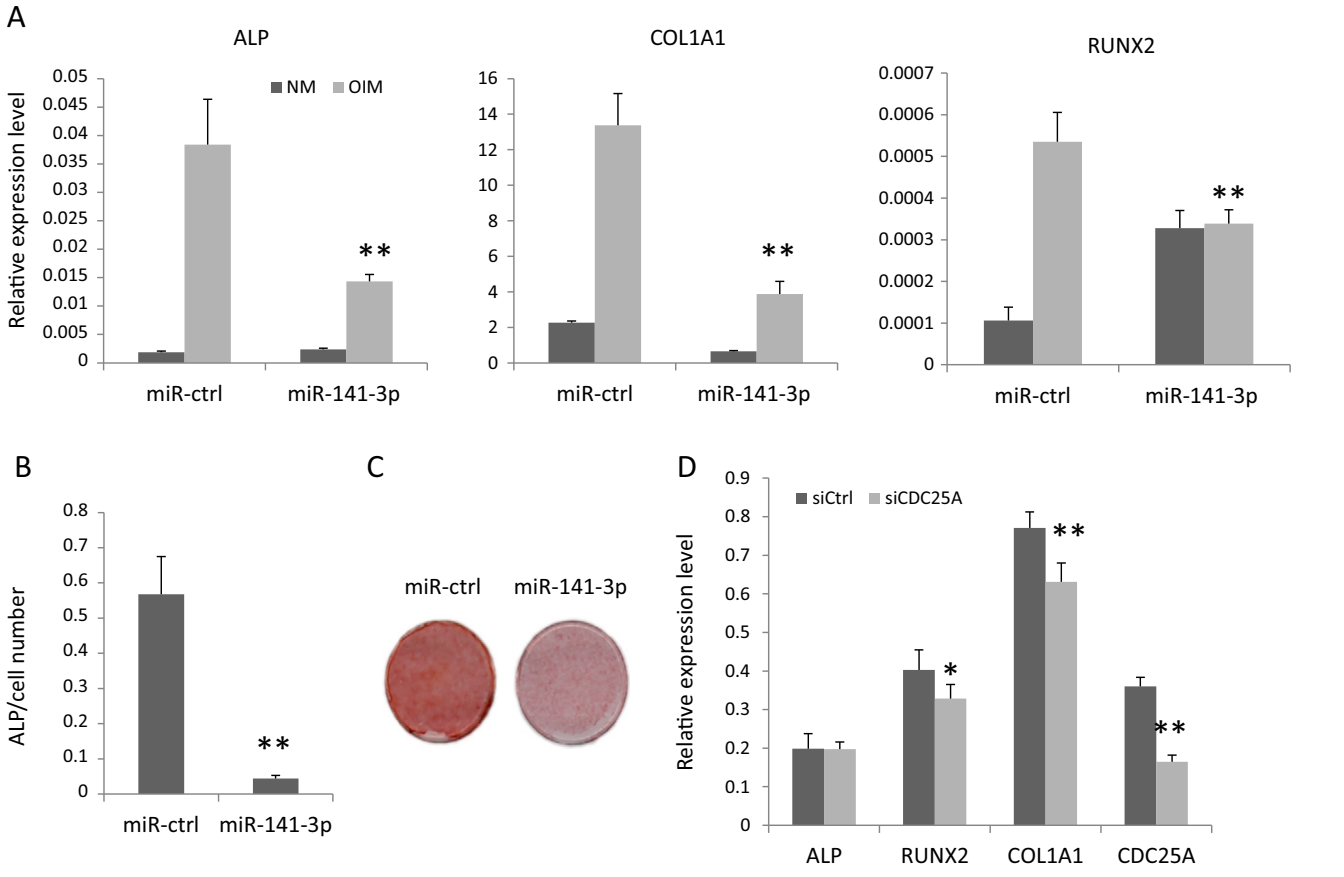

Fig. 6. miR-141 inhibits in vitro osteoblast differentiation of hMSC. (A–C) hMSC was reverse transfected with 9 nM control miRNA (miR-ctrl) or miR-141-3p and cultured in normal medium (NM) or osteogenic induction medium (OIM) for 4–13 days. The expression of osteoblastic markers was analyzed by real-time qRT-PCR and normalized against GAPDH. Data are shown as mean + S.D., n = 6, **P < 0.005 comparing to miR-ctrl plus OIM (A). ALP activity was quantitated at day 7 and normalized against cell number. Data are shown as mean + S.D., n = 8. **P < 0.005 (B). In vitro mineralization was determined by alizarin red staining on day 13 (C). (D) hMSC were reverse transfected with 33 nM control siRNA (siCtrl) or siRNA targeting CDC25A (siCDC25A) followed by osteoblast differentiation for 7 days. The expression of osteoblastic markers was analyzed by real-time qRT-PCR and normalized against GAPDH. Data are shown as mean + S.D., n = 6. *P < 0.05, **P < 0.005.

was not as pronounced as observed in miR-141-3p overexpression, possibly due the functional rescue by CDC25B or CDC25C [29]. This notion is supported by evidence that biological effects of CDC25A deficiency was rescued by CDC25B in adult mice deficient in the CDC25A gene [37,38].

It is plausible that there exist other proteins that are targeted by miR-141-3p and mediate its effect on hMSC proliferation and differentiation. We observed that miR-141-3p inhibited Wnt signaling and Wnt3a induced ALP activity. Searching TarBase [28] for known targets of miR-141-3p, we identified Wnt target gene CCND1 [30] as the only miR-141-3p target involved in Wnt signaling. Upregulation of CCND1 by miR-141-3p could not explain the miR-141 inhibitory effect on Wnt signaling. By screening miR-141-3p targeting sites in Wnt signaling genes (http://www.stanford.edu/group/nusselab/cgi-bin/wnt/) using the microRNA.org web resource [25], five Wnt genes: WNT5A, WNT16, FZD8, APC2 and AXIN1 were predicated to have one miR-141-3p target site (Supplemental Table 2). WNT16, APC2 and AXIN1 are not expressed in hMSC [15]. For FZD8, no miR-141-3p targeting site was detected by two additional predication tools (TargetScan and PicTar). The same targeting site of miR-141-3p in WNT5A was also predicated by TargetScan, but this Wnt ligand was normally regarded as noncanonical Wnt ligand. Thus, bioinformatics analysis did not provide insight into how miR-141-3p inhibited Wnt signaling. Whether miR-141-3p inhibits Wnt signaling directly or indirectly needs to be explored.

In summary, our results provide new insight into the interaction of Wnt signaling and miRNAs in hMSC proliferation and differentiation. As a regulator of hMSC proliferation and differentiation, targeting miR-141-3p could be a novel anabolic therapy for bone loss diseases, e.g. osteoporosis.

Supplementary data to this article can be found online at http://dx.doi.org/10.1016/j.bbamcr.2014.06.004.

Acknowledgement

We thank Linda Harkness for proof reading. This work was supported by grants from Fabrikant Vilhelm Pedersen og Hustrus, Novo Nordisk Foundation, a local grant from Odense University Hospital.

References

[1] L. He, G.J. Hannon, MicroRNAs: small RNAs with a big role in gene regulation, Nat. Rev. Genet. 5 (2004) 522–531.
[2] H. Taipaleenmaki, L. Bjerre Hokland, L. Chen, S. Kauppinen, M. Kassem, Mechanisms in endocrinology: micro-RNAs: targets for enhancing osteoblast differentiation and bone formation, Eur. J. Endocrinol. 166 (2012) 359–371.
[3] L.P. Lim, N.C. Lau, P. Garrett-Engele, A. Grimson, J.M. Schelter, J. Castle, D.P. Bartel, P.S. Linsley, J.M. Johnson, Microarray analysis shows that some microRNAs downregulate large numbers of target mRNAs, Nature 433 (2005) 769–773.
[4] A. Kozomara, S. Griffiths-Jones, miRBase: integrating microRNA annotation and deep-sequencing data, Nucleic Acids Res. 39 (2011) D152–D157.
[5] P.H. Olsen, V. Ambros, The lin-4 regulatory RNA controls developmental timing in Caenorhabditis elegans by blocking LIN-14 protein synthesis after the initiation of translation, Dev. Biol. 216 (1999) 671–680.
[6] G. Hutvagner, P.D. Zamore, A microRNA in a multiple-turnover RNAi enzyme complex, Science 297 (2002) 2056–2060.
[7] C. Llave, Z. Xie, K.D. Kasschau, J.C. Carrington, Cleavage of Scarecrow-like mRNA targets directed by a class of Arabidopsis miRNA, Science 297 (2002) 2053–2056.
[8] B.A. Janowski, S.T. Younger, D.B. Hardy, R. Ram, K.E. Huffman, D.R. Corey, Activating gene expression in mammalian cells with promoter-targeted duplex RNAs, Nat. Chem. Biol. 3 (2007) 166–173.
[9] B. Khraiwesh, M.A. Arif, G.I. Seumel, S. Ossowski, D. Weigel, R. Reski, W. Frank, Transcriptional control of gene expression by microRNAs, Cell 140 (2010) 111–122.
[10] J.B. Lian, G.S. Stein, A.J. van Wijnen, J.L. Stein, M.Q. Hassan, T. Gaur, Y. Zhang, MicroRNA control of bone formation and homeostasis, Nat. Rev. Endocrinol. 8 (2012) 212–227.
[11] T. Eskildsen, H. Taipaleenmaki, J. Stenvang, B.M. Abdallah, N. Ditzel, A.Y. Nossent, M. Bak, S. Kauppinen, M. Kassem, MicroRNA-138 regulates osteogenic differentiation of human stromal (mesenchymal) stem cells in vivo, Proc. Natl. Acad. Sci. U. S. A. 108 (2011) 6139–6144.
[12] T. Eguchi, K. Watanabe, E.S. Hara, M. Ono, T. Kuboki, S.K. Calderwood, OstemiR: a novel panel of microRNA biomarkers in osteoblastic and osteocytic differentiation from mesencymal stem cells, PLoS One 8 (2013) e58796.
[13] B.M. Abdallah, M. Kassem, Human mesenchymal stem cells: from basic biology to clinical applications, Gene Ther. 15 (2008) 109–116.
[14] J.M. Gimble, S. Zvonic, Z.E. Floyd, M. Kassem, M.E. Nuttall, Playing with bone and fat, J. Cell. Biochem. 98 (2006) 251–266.
[15] W. Qiu, T.E. Andersen, J. Bollerslev, S. Mandrup, B.M. Abdallah, M. Kassem, Patients with high bone mass phenotype exhibit enhanced osteoblast differentiation and inhibition of adipogenesis of human mesenchymal stem cells, J. Bone Miner. Res. 22 (2007) 1720–1731.
[16] K. Kapinas, C.B. Kessler, A.M. Delany, miR-29 suppression of osteonectin in osteoblasts: regulation during differentiation and by canonical Wnt signaling, J. Cell. Biochem. 108 (2009) 216–224.
[17] Z. Li, M.Q. Hassan, M. Jafferji, R.I. Aqeilan, R. Garzon, C.M. Croce, A.J. van Wijnen, J.L. Stein, G.S. Stein, J.B. Lian, Biological functions of miR-29b contribute to positive regulation of osteoblast differentiation, J. Biol. Chem. 284 (2009) 15676–15684.
[18] K. Kapinas, C. Kessler, T. Ricks, G. Gronowicz, A.M. Delany, miR-29 modulates Wnt signaling in human osteoblasts through a positive feedback loop, J. Biol. Chem. 285 (2010) 25221–25231.
[19] T. Wang, Z. Xu, miR-27 promotes osteoblast differentiation by modulating Wnt signaling, Biochem. Biophys. Res. Commun. 402 (2010) 186–189.
[20] J. Zhang, Q. Tu, L.F. Bonewald, X. He, G. Stein, J. Lian, J. Chen, Effects of miR-335-5p in modulating osteogenic differentiation by specifically downregulating Wnt antagonist DKK1, J. Bone Miner. Res. 26 (2011) 1953–1963.
[21] J.L. Simonsen, C. Rosada, N. Serakinci, J. Justesen, K. Stenderup, S.I. Rattan, T.G. Jensen, M. Kassem, Telomerase expression extends the proliferative life-span and maintains the osteogenic potential of human bone marrow stromal cells, Nat. Biotechnol. 20 (2002) 592–596.
[22] M. Al-Nbaheen, R. Vishnubalaji, D. Ali, A. Bouslimi, F. Al-Jassir, M. Megges, A. Prigione, J. Adjaye, M. Kassem, A. Aldahmash, Human stromal (mesenchymal) stem cells from bone marrow, adipose tissue and skin exhibit differences in molecular phenotype and differentiation potential, Stem Cell Rev. 9 (2013) 32–43.
[23] W. Qiu, Y. Hu, T.E. Andersen, A. Jafari, N. Li, W. Chen, M. Kassem, Tumor necrosis factor receptor superfamily member 19 (TNFRSF19) regulates differentiation fate of human mesenchymal (stromal) stem cells through canonical Wnt signaling and C/EBP, J. Biol. Chem. 285 (2010) 14438–14449.
[24] W. Qiu, L. Chen, M. Kassem, Activation of non-canonical Wnt/JNK pathway by Wnt3a is associated with differentiation fate determination of human bone marrow stromal (mesenchymal) stem cells, Biochem. Biophys. Res. Commun. 413 (2011) 98–104.
[25] D. Betel, M. Wilson, A. Gabow, D.S. Marks, C. Sander, The microRNA.org resource: targets and expression, Nucleic Acids Res. 36 (2008) D149–D153.
[26] A. Krek, D. Grun, M.N. Poy, R. Wolf, L. Rosenberg, E.J. Epstein, P. MacMenamin, I. da Piedade, K.C. Gunsalus, M. Stoffel, N. Rajewsky, Combinatorial microRNA target predictions, Nat. Genet. 37 (2005) 495–500.
[27] B.P. Lewis, C.B. Burge, D.P. Bartel, Conserved seed pairing, often flanked by adenosines, indicates that thousands of human genes are microRNA targets, Cell 120 (2005) 15–20.
[28] T. Vergoulis, I.S. Vlachos, P. Alexiou, G. Georgakilas, M. Maragkakis, M. Reczko, S. Gerangelos, N. Koziris, T. Dalamagas, A.G. Hatzigeorgiou, TarBase 6.0: capturing the exponential growth of miRNA targets with experimental support, Nucleic Acids Res. 40 (2012) D222–D229.
[29] R. Boutros, V. Lobjois, B. Ducommun, CDC25 phosphatases in cancer cells: key players? Good targets? Nat. Rev. Cancer 7 (2007) 495–507.
[30] L. Zhang, T. Deng, X. Li, H. Liu, H. Zhou, J. Ma, M. Wu, M. Zhou, S. Shen, Z. Niu, W. Zhang, L. Shi, B. Xiang, J. Lu, L. Wang, D. Li, H. Tang, G. Li, microRNA-141 is involved in a nasopharyngeal carcinoma-related genes network, Carcinogenesis 31 (2010) 559–566.
[31] M. Korpal, Y. Kang, The emerging role of miR-200 family of microRNAs in epithelial-mesenchymal transition and cancer metastasis, RNA Biol. 5 (2008) 115–119.
[32] N.E. Renthal, K.C. Williams, C.R. Mendelson, MicroRNAs–mediators of myometrial contractility during pregnancy and labour, Nat. Rev. Endocrinol. 9 (2013) 391–401.
[33] D.M. Dykxhoorn, Y. Wu, H. Xie, F. Yu, A. Lal, F. Petrocca, D. Martinvalet, E. Song, B. Lim, J. Lieberman, miR-200 enhances mouse breast cancer cell colonization to form distant metastases, PLoS One 4 (2009) e7181.
[34] Y. Du, Y. Xu, L. Ding, H. Yao, H. Yu, T. Zhou, J. Si, Down-regulation of miR-141 in gastric cancer and its involvement in cell growth, J. Gastroenterol. 44 (2009) 556–561.
[35] X.Y. Yu, Z. Zhang, J. Liu, B. Zhan, C.Z. Kong, MicroRNA-141 is downregulated in human renal cell carcinoma and regulates cell survival by targeting CDC25B, Oncol. Targets Ther. 6 (2013) 349–354.
[36] T. Itoh, Y. Nozawa, Y. Akao, MicroRNA-141 and -200a are involved in bone morphogenetic protein-2-induced mouse pre-osteoblast differentiation by targeting distal-less homeobox 5, J. Biol. Chem. 284 (2009) 19272–19279.
[37] G. Lee, L.S. White, K.E. Hurov, T.S. Stappenbeck, H. Piwnica-Worms, Response of small intestinal epithelial cells to acute disruption of cell division through CDC25 deletion, Proc. Natl. Acad. Sci. U. S. A. 106 (2009) 4701–4706.
[38] G. Lee, S. Origanti, L.S. White, J. Sun, T.S. Stappenbeck, H. Piwnica-Worms, Contributions made by CDC25 phosphatases to proliferation of intestinal epithelial stem and progenitor cells, PLoS One 6 (2011) e15561.